Subscripts

0 = inlet of heating
c = critical condition
w = wall, lower boundary

Superscripts

— = undisturbed phase
* = perturbed phase
** = amplitude of the disturbances

LITERATURE CITED

Chandra, K., "Instability of Fluids Heated from Below," *Proc. Roy. Soc.*, **A164**, 231 (1938).

Chandrasekhar, S., *Hydrodynamic and Hydromagnetic Stability*, Oxford, Clarendon Press (1961).

Currie, I. G., "The Effect of Heating Rate on the Stability of Stationary Fluids," *J. Fluid Mech.*, **20**, 337 (1967).

Deardorff, J. E., "Gravitational Instability Between Horizontal Plates with Shear," *Physics Fluids*, **8**, 1027 (1965).

Foster, T. D., "Onset of Convection in a Layer of Fluid Cooled from Above," *ibid.*, **8**, 1770 (1965).

Frisk, D. P., and E. J. Davis, "The Enhancement of Heat Transfer by Waves in Stratified Gas-Liquid Flow," *Intern. J. Heat Mass Transfer*, **15**, 1537 (1972).

Gallagher, A. P., and A. McD. Mercer, "On the Behavior of Small Disturbances in Plane Couette Flow with a Temperature Gradients," *Proc. Roy. Soc.*, **A286**, 117 (1965).

Goldstein, A. W., "Stability of a Horizontal Fluid Layer with Unsteady Heating from Below and Time-Dependent Body Force," *NASA Tech. Report*, R-4 (1959).

Gresho, P. M., and R. L. Sani, "The Stability of a Fluid Layer Subjected to a Step Change in Temperature," *Intern. J. Heat Mass Transfer*, **14**, 207 (1971).

Lick, W., "The Instability of a Fluid Layer with Time-Dependent Heating," *J. Fluid Mech.*, **21**, 565 (1965).

Morton, B. R., "On the Equilibrium of a Stratified Layer of Fluid," *J. Mech. Appl. Math.*, **10**, 433 (1957).

Rayleigh, L., "On Convection Currents in a Horizontal Layer of Fluid when the Higher Temperature is on the Under Side," *Phil. Mag.*, **32**, 529 (1916).

Manuscript received June 21, 1973, and accepted September 19, 1973.

Pore Accessibility Applied to Correction of Errors in Mercury Porosimetry

GREGORY P. WOTZAK

Division of Fluid, Chemical, and Thermal Processes
Rensselaer Polytechnic Institute, Troy, New York 12181

Characterization of the structure of porous materials is often necessary for an understanding of the properties and behavior of these materials in such varied applications as catalysis, fuel cells, secondary oil recovery, etc. Traditionally, porosity and pore size distributions have been important measures of pore structure conveniently determined by mercury penetration porosimetry. However, researchers have begun to inquire concerning the accuracy of mercury porosimetry, as well as possible alternate means for quantification of pore structure. This note presents a flexible, general method for the correlation and correction of distortions in porosimetry measurements and advances the concept of pore accessibility as an important characteristic of pore structure.

Mercury intrusion porosimetry inherently introduces errors into the determination of pore size distributions. It will not account for pores which can only be entered through pores or necks narrower than the pore itself. Intruded volumes of these pores are incorrectly assigned to the radii of smaller pores leading to these partially accessible pores. The extent of these errors appear to be dependent on sample size. A thin sample will have most of these larger pores easily accessible to the sample surface while a thick sample will have many large pores buried deep within the pore structure.

Meyer (1953) developed a probability-based method to correct errors introduced by these partially accessible pores. Kzenyhek (1963) expanded on the earlier work of Fatt (1956) in an effort to produce a more generalized correction method which took into account the size of the porous sample. The present work advances the approaches of Kzenyhek and Fatt such that distributions of pore length and the number of pore which connect at pore junctions are included in a generalized approach to correction of porosimeter data.

SYSTEM MODEL

Stochastic simulations of mercury intrusion porosimetry were performed in order to determine the sensitivity of errors in pore size distributions to: (1) shape of the actual pore size distribution, (2) sample size, (3) variations of pore length with pore radius, and (4) average number of pores which meet at a pore intersection. For simplicity, various beta distributions (Greenkorn and Kessler, 1969) were used to assess the influence of the shape of the pore size distribution. Pore lengths were related to pore radii by means of an inverse power relationship suggested by Fatt (1956):

$$l = l_0\, r^{-\alpha} \qquad \alpha \geqq 0$$

A two-pass computer program was used to simulate contributions of primary pores to the mercury penetration volume. Large numbers of mercury slugs were initiated at the appropriate sample face and were followed through the pore structure as a function of increasing mercury pressure. At junctions of pores, random numbers were utilized in order to determine the orientation, radius, and length of the most probable pore for mercury penetration at the current system pressure. A self-normalizing routine based on an isotropic distribution of pore directions was used to determine the spatial position of the next pore junction. The average pore length was chosen as the spatial unit in the direction normal to the sample face. A second pass through the porous material was necessary in order to account for spatial interference of mercury slugs within the simulated sample. Typical computational times were 15 to 30 min. on an IBM 360/50 computer.

Output from the stochastic program was smoothed and normalized by a second program. Local mercury saturations of primary or active pores indicate the accessibility of secondary pores to the advancing mercury front. Resulting mercury saturations of these secondary pores are combined with primary pore saturations to yield intruded volume as a function of mercury pressure. Output of the final program also includes apparent pore size distribution errors associated with the presence of partially inaccessible pores.

MODEL RESULTS

Evaluation of simulation results indicate that a generalized correction function can be used to correlate and predict errors in pore size distributions resulting from the presence of large pores deep within the porous medium. For a given reduced sample thickness, a normalized correction correlation was found to satisfy the pore size distributions error function. In addition, the sensitivity of errors in pore size distributions to various properties of porous materials has been determined.

Trends in the correction function are illustrated by Figure 1. The penetration error represents the difference between mercury intrusion for an ideal, totally accessible sample and the apparent mercury penetration for the actual test specimen. This penetration error is given

$$\epsilon = \int_{r_{\max}}^{r} [D(r')_{\text{true}} - D(r')_{\text{apparent}}]\, dr'$$

Generalized correlations are presented by use of a reduced penetration error defined as

$$E = \frac{\epsilon}{\epsilon_m}$$

where ϵ_m is the maximum value of penetration error corresponding to the limiting case of an infinitely thick sample. In order to present the most generalized correlations possible, apparent penetration has been used as the independent variable in Figure 1, such that

$$\rho = \int_{r_{\max}}^{r} D(r')_{\text{apparent}}\, dr'$$

The reduced thickness is defined by

$$D = \frac{d}{d_0}$$

where d_0 is a characteristic length which is a function of porous material structure. A reduced relative maximum error is defined

$$E' = \frac{\epsilon'}{\epsilon_m}$$

where ϵ' is the relative maximum penetration error for a given sample thickness.

Values of ϵ_m and d_0 for a particular porous material are functions of characteristic properties of that substance. Within the framework of the system model, eight different simulated porous materials were studied in order to determine the sensitivity of maximum penetration error and characteristic length to particular material properties. System parameters varied in this evaluation included: (1) shape of the true pore size distribution as represented by a particular beta distribution, (2) relationship between pore length and pore radius as defined by a value of the inverse power α, (3) breadth of a pore size distribution of a given shape, and (4) characteristic average number of pores at a pore junction. A detailed analysis of simulation results indicates that the maximum penetration error is a strong inverse function of the average number of pores per junction and varies inversely in a secondary manner with the power factor α. Characteristic length d_0 has been found to be inversely proportional to the breadth of the pores size distribution and decreases in magnitude as the pores size distribution becomes more skewed towards larger pores. A measure of the influence of the number of pores at a junction or maximum penetration error is provided by selected model results. For $\alpha = 1.0$, porous material simulations indicated that $\epsilon_m = 0.68$ for the case of 5 pores at a pore junction while 13 pores at a junction resulted in a value of $\epsilon_m = 0.34$.

COMPARISON WITH LITERATURE RESULTS

Figure 1 and its crossplots can be used to correlate and predict errors in mercury porosimetry. Joyner and

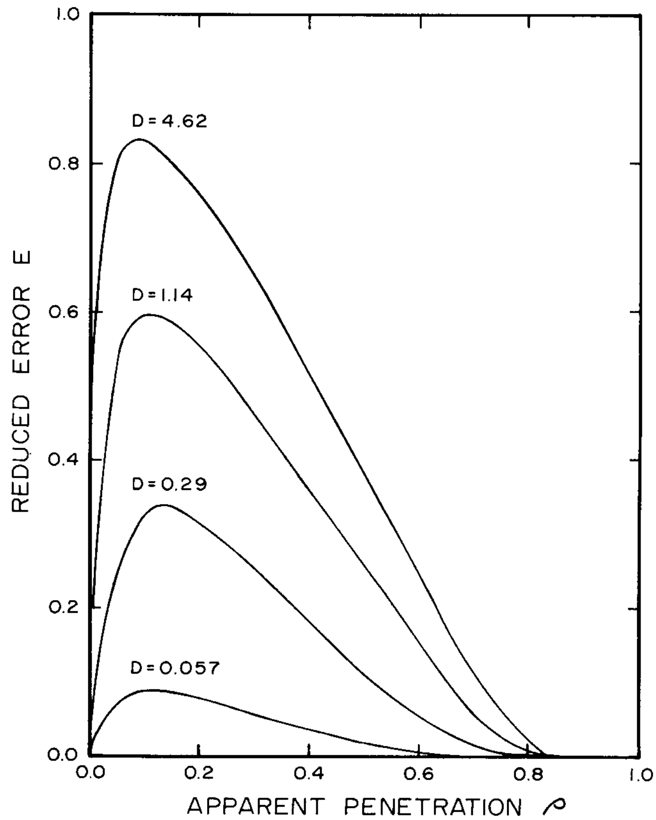

Fig. 1. Reduced correction function for selected reduced sample thicknesses.

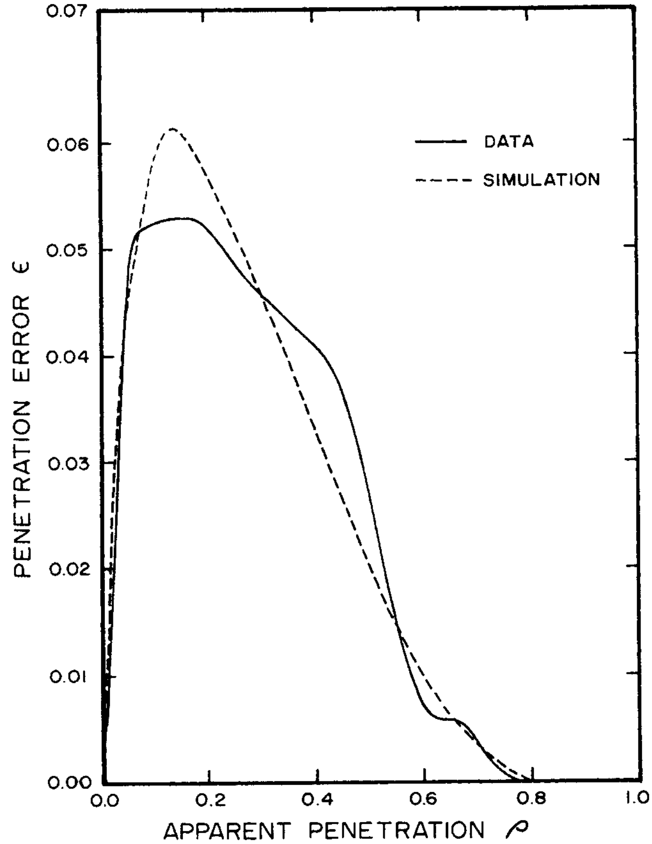

Fig. 2. Comparison of model results with data of Joyner et al.

co-workers (1951) measured pore size distributions of different samples by both capillary condensation and mercury porosimetry. Results of the condensation method provides a reasonable measure of the true pore size distribution since the technique is not significantly influenced by pore inaccessibility. Comparison of model predictions with experimental results of Figure 4a of the Joyner article is illustrated by Figure 2. The correlations between model and experimental results implies the following system parameters: $\epsilon = 0.06$, $\epsilon_m = 0.18$, $E' = 0.34$, and $D = 0.29$. The small 6% penetration error indicates that the test specimen is thin enough for mercury porosimetry to yield an accurate pore size distribution.

The system model presented in this note also has predictive power. Porosimeter data for different sample sizes of a given material can be utilized to back-calculate the true pore size distribution. Results presented in Figure 4 of the work of Reich (1967) have been analyzed by use of crossplots of Figure 1. Specimen thicknesses of 5, 10, and 15 millimeters correspond approximately to reduced thicknesses of 5.1, 10.2, and 15.3. A relative maximum penetration error of 0.38 predicted for the 5-mm sample is comparable to the maximum penetration error of 0.48. Therefore, mercury porosimetry results for even this thin sample appears to be significantly in error. An apparent volume average pore radius of 40 microns (5-mm sample) is significantly different from a model prediction of 180 microns.

Similar disagreements were found by Dullien and Mehta (1970) in their comparison of pore size distributions obtained from a photomicrographic method and mercury porosimetry. The more exact photomicrographic analysis of a Woods metal matrix yielded an average pore radius of 200 microns while mercury porosimetry indicated a 40-micron average pore radius. Pore size distributions obtained by Svata and Zabransky (1968) with a sedimentation balance method indicated that average pore radii obtained for sintered silver samples were approximately twice that predicted by porosimetry results.

CONCLUSIONS

Correlation and prediction methods presented in this note accent the role of pore accessibility as a primary mechanism for the introduction of errors into mercury porosimetry. Trends indicated by the system model are consistent with intuitive and experimental evidence. The average number of pores at a pore junction have been shown to play a critical role in determining the maximum possible penetration error.

Specification of an accessibility factor in addition to the porosity and pore size distribution of a sample provides a more complete characterization of the properties and behavior of a porous material. Development of a workable definition of such an accessibility factor, as well as the implications of this factor in porous system behavior, will be the subject of further research specifically directed towards fuel cell systems.

ACKNOWLEDGMENT

This work was sponsored by the Department of Defense under contract number DAAB07-69-C-0063.

NOTATION

d = sample thickness
d_0 = characteristic length of material
D = reduced sample thickness
$D(r)_{\text{apparent}}$ = apparent pore size distribution
$D(r)_{\text{true}}$ = true pore size distribution
E = reduced penetration error
E' = reduced relative maximum error
l = pore length
l_0 = pore length proportionality factor
r = pore radius
α = length inverse power factor
ϵ = penetration error
ϵ_m = maximum penetration error
ϵ' = relative maximum penetration error
ρ = apparent penetration

LITERATURE CITED

Dullien, F. A., and V. K. Batra, "Determination of the Structure of Porous Media," *Ind. Eng. Chem.*, **62**, 25 (1970).

Fatt, I., "The Network Model of Porous Media," *Trans. AIME*, **207**, 144 (1956).

Greenkorn, R. A., and D. P. Kessler, "Dispersion in Heterogeneous Nonuniform Anisotropic Porous Media," *Ind. Eng. Chem.*, **61**, 14 (1969).

Joyner, L. G., E. P. Barret, and R. Skold, "The Determination of Pore Volume and Area Distributions in Porous Substances II," *J. Am. Chem. Soc.*, **73**, 3155 (1951).

Ksenzhek, O. S., "Capillary Equilibrium in Porous Media with Intersecting Pores," *Russ. J. Phys. Chem.*, **37**, 691 (1963).

Meyer, H. I., "Pore Distributions in Porous Media," *J. Appl. Phys.*, **24**, 510 (1953).

Reich, B., "The Determination of Pore Size Distributions in Large Pore Materials by Use of Mercury Porosimetry," *Chem. Ing. Techn.*, **39**, 1275 (1967).

Svata, M., and Z. Zabransky, "Determination of Pore Size Distribution Using a Sedimentation Balance," *Powder Tech.*, **2**, 159 (1968).

Manuscript received September 7, 1973, and accepted October 15, 1973.